www.czasopisma.pan.pl PAN POLSKA AKADEMIA NAUK www.journals.pan.pl

Arch. Metall. Mater. **67** (2022), 4, 1283-1291

DOI: https://doi.org/10.24425/amm.2022.141053

CHANGZHUANG ZHOU[1], LIN MA[1,2*], CHAO ZHU[1], QINGHE CUI[1], JINDI LIANG[1], YUJIAN SONG[1]

THE EFFECT OF POWER ULTRASOUND ON MICROSTRUCTURE EVOLUTION DURING THE TRANSIENT LIQUID STAGE OF ULTRASONIC-PROMOTED TLP BONDING SiCp/Al MMCs

Ultrasound-promoted transient liquid phase bonding (U-TLP) is a high quality, high efficiency, and low-cost method for fast bonding of difficult-wetting materials in the atmospheric environment. In this paper, U-TLP was used to bond SiC particles reinforced aluminium-based metal matrix composite which particle volume fraction was 70%. The pure zinc foil was used as the intermediate layer. The effects of ultrasonic on microstructure evolution and mechanical properties of joints during the transient liquefaction stage were investigated. The mechanism of ultrasonic effects in the transient liquefaction stage of U-TLP was also inducted. The results showed that high volume fraction SiCp/Al MMCs were bonded well at low temperature in the air environment. Ultrasonic vibration can remove the oxide film on the surface of aluminum matrix composites, enhance the wettability of SiC particles with weld metal, promote atomic diffusion and homogenization of SiC particles, and improve the welding quality and efficiency. Reasonable increase of ultrasonic vibration time could effectively improve the joint strength.

Keywords: Transient liquid phase bonding; Silicon carbide reinforced aluminum matrix composites; Ultrasonics; Zinc interlayer

1. Introduction

SiC particle reinforced Al-based metal matrix composites (SiCp/Al MMCs) have developed rapidly in recent years due to their excellent properties such as high elastic modulus and low thermal expansion coefficient [1,2]. SiCp/Al MMCs have been broadly used in electronic packaging [1], aerospace industry [2], and other fields [2]. The bonding technology of SiCp/Al MMCs is one of the keys to expand the application field of Si/Al MMCs. Some welding methods are currently used to bonding SiCp/Al MMCs such as fusion welding, friction stir welding, brazing, and diffusion welding. Fusion welding is one of the most common bonding methods, while SiC in SiCp/Al MMCs is easy to react with aluminum and form brittle phase Al_4C_3 in a high welding temperature. The brittle Al_4C_3 easily resulted in a decrease in joint strength [3-18]. Brazing, friction stir welding, and diffusion welding could form joint in low temperature and avoid the formation of Al_4C_3 [7,8,10,11,14]. Friction stir welding was difficult to achieve large areas bonding. Although brazing could bond large plates, the solder's strength was usually much lower than the base metal [9,17,19,20].

Transient Liquid Phase (TLP) bonding was developed based on diffusion welding. Compared with traditional welding methods, TLP was more suitable for bonding Si/Al MMCs because of relatively low temperature and low pressure. The TLP bonding process was composed of two steps as follows. (1) Transient liquefaction stage. The interlayer material diffuses with the substrate to form eutectic, which melting point is lower than interlayer metal. The eutectic with a low melting point liquefies at the bonding temperature. This local liquid area promotes the dissolution and diffusion between the base material and interlayer. Within a short time, the interlayer is completely liquefied. (2) Isothermal solidification stage. In this stage, the elements of base metal dissolve into the liquid zone at a constant temperature. The components of the bonding zone change and depart from the eutectic component gradually. The bonding area solidifies and finally forms a uniform metallurgical joint after element homogenizing for a certain time. Currently, several metals have been used as the intermediate layer to bond Al MMCs, such as copper, nickel, silver foil, etc. [21,22]. However, the following issues still exist when bonding SiCp/Al MMCs by TLP. First, the vacuum environment is required to decompose and remove

[1] SHENYANG AEROSPACE UNIVERSITY, SCHOOL OF MATERIALS SCIENCE AND ENGINEERING, SHENYANG 110136, CHINA
[2] THE UNIVERSITY OF QUEENSLAND, AUSTRALIA

* Corresponding author: linma@sau.edu.cn

the oxide film on base metal and interlayer surfaces. The strict requirement for vacuum increases the cost and limits the use of some easily evaporating metal as the interlayer, such as Zn alloy and Mg alloy. Secondly, the interface wettability between SiC particles and aluminum alloy is poor, which affects the quality of the interface bonding [23]. Thirdly, according to the crystallization growth principle, The SiC particles, which migrated into the bonding area, locate at the grain boundary. That inevitably produces particle segregation, which significantly affects the bonding joint's mechanical properties [24,25]. Besides, the TLP process takes a long time (tens of minutes to several hours) to obtain a uniform microstructure joint.

To solve the problems in conventional TLP, a new bonding technology combined ultrasound and TLP appeared, named Ultrasonic-promoted Transient liquid Phase bonding (U-TLP). Currently, the U-TLP has been used to bond magnesium alloys and Al-Si alloys [26-28]. AZ31B magnesium alloy was successfully bonded in 1 s by UTLP in the atmospheric environment with pure Zn interlayer [27]. Magnesium alloy was well bonded by U-TLP with Cu foil and Zn foil as the interlayer at 460°C and 370°C, respectively. The maximum shear strength of the joint reached 105 MPa, which was basically equal to the base metal's strength [28]. Al-50 Si alloy was bonded well by U-TLP at 390°C in the air with a pure zinc interlayer. With applying ultrasonic vibration for 128 s, the Si particle reinforced Zn-Al matrix composite joint was formed. The shear strength of the joint was 94.2 MPa, while, a thin Zn-Al eutectic layer and local particles segregation still existed at that time. Besides, the ultrasonic vibration duration also influenced the distribution of Si particles. [26]. In the process of U-TLP, ultrasound mainly worked in the transient liquefaction stage (TLS). The mechanism of ultrasonic effects in TLS was the key to understand U-TLP. In the TLS, the effects of ultrasonic included breaking down the oxide film and promoting element dissolution and diffusion. The first effect was breaking the oxide film [29,30]. In U-TLP, there is a hard contact stage between solid phase (oxide film of the substrate) and solid phase (oxide film of interlayer metal) before the formation of the liquid phase, which was different from ultrasonic-assisted brazing [31]. The rupture of oxide film during the hard contact stage was a prerequisite for the formation of the eutectic liquid phase via atomic diffusion. Secondly, the degree of atomic diffusion was one of the important factors which affected the bonding strength. Ultrasound has been proved to accelerate the diffusion and dissolution of atoms [32]. For the bonding process of high volume SiCp/Al MMCs, however, the blocking effect of SiC particles near the interface may affect the promoting effect of ultrasound on atomic diffusion. Besides, the mixture effect of acoustic flow was approved to promote particle homogenization in the brazing process of SiCp/Al MMCs [32]. However, there is still a question of whether ultrasound can significantly decrease SiC particles' segregation during the short time of the transient liquefaction stage.

In this paper, U-TLP was used to bond a high-volume-fraction (70%) SiCp/Al MMCs with pure Zn interlayer in the air at low-temperature in the air. The main aim was to explore the mechanism of ultrasonic effects in the transient liquefaction stage of U-TLP. The effects of ultrasound on oxide film breaking down, atomic diffusion, and SiC particles migration in U-TLP were investigated in details. Finally, the physical process models of the transient liquefaction stage of U-TLP was established.

2. Materials and methods

70 vol% SiC particles reinforced 6061Al based MMCs were used as the base material. The shear strength of the base material was 150.2 MPa. Fig. 1 shows the microstructure of the base material. There were three kinds of SiC particles in the composite material, i.e. the mini-size one, the middle-size one, and the large-size one. The particles' diameters were around 1 ~ 5 μm, 10 ~ 20 μm, 40 ~ 50 μm. The base composites were cut into specimens with dimensions of 10 mm × 6 mm × 3 mm. Pure Zn foils with a thickness of 50 μm were used as the interlayer. Before bonding, the specimens and pure Zn foils were ground to 1200 grit on SiC papers and then cleaned in acetone and alcohol by ultrasonic cleaner for 20 min.

The schematic diagram of U-TLP bonding is shown in Fig. 2. The composite materials and the Zn interlayer were constructed as a sandwich and then were heated to the bonding temperature. The temperature was measured by thermocouple during the whole bonding process. Based on the principle of transient liquid diffusion bonding, the bonding temperature in this paper was set at 390°C, which was slightly higher than the melting point of Zn-Al eutectic but lower than the melting point of pure Zn interlayer. When the specimen's temperature was elevated to the bonding temperature, A constant pressure of 1.5 Mpa was applied through the ultrasonic horn to ensure the close contact between the base materials and interlayer. Subsequently, when the specimen's temperature was stable at 390°C, ultrasonic vibration was applied on the top of the fixture for different durations (2 ~ 60 s). The ultrasonic frequency was 20 kHz and the power was 2 kW. The ultrasonic horn was immediately removed after applying. Then the specimens were quenched in 0°C water, instantly.

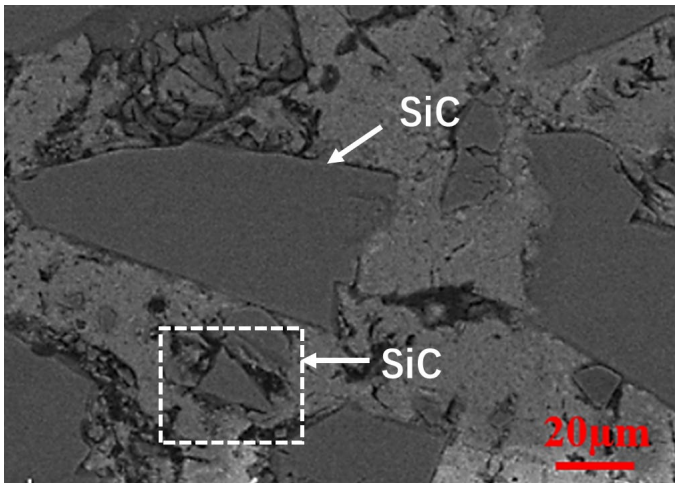

Fig. 1. Original microstructure of Al MMCs

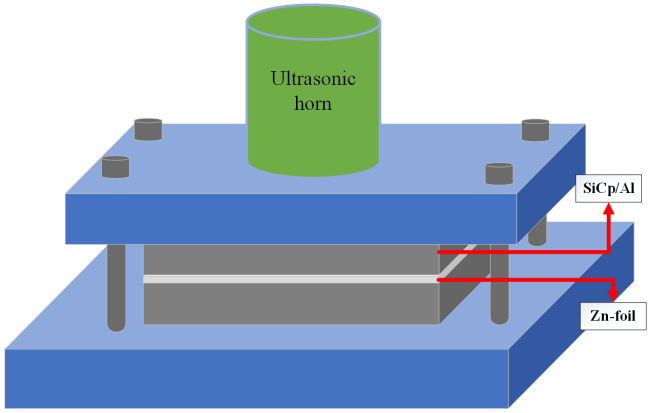

Fig. 2. The schematic diagram of the U-TLP bonding process

After bonding, the cross-sections of the joints were grounded and mechanical polished. SEM (Scanning electron microscope, Fei-Quanta 200F) was used to analyze the microstructure and the EDX (energy dispersive X-Ray spectrometer) was used to identify the composition of the bonding area. The shear strength test was conducted by Instron 8801 tensile testing machine and the schematic diagram of the tensile shear strength test is shown in Fig. 3. The size of the shear test specimen was 10 mm×6 mm×6 mm and the stress loading speed was 1 mm/min. To ensure the reliability of the value measured in the shear test, at least three specimens were tested for each experimental parameter and the average values were obtained. The fracture morphology of the joints was observed by SEM.

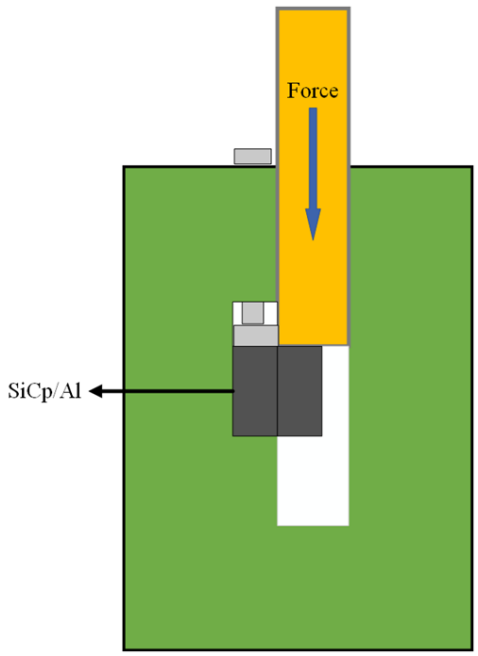

Fig. 3. The schematic diagram of the shear strength test

3. Results

The overall cross-section morphology and local microstructure of U-TLP joints of SiCp/Al MMCs with different ultrasonic duration are shown in Figs 4 and 5. In the previous work, the extrusion effect of ultrasonic vibration has been certified and investigated in detail [33]. The blocking effect of SiC particles caused the irregular shape of the dissolution zone. To investigate the effect of ultrasound on promoting element dissolution in the transient liquid period, considering the extrusion effect of ultrasound, the mean values of dissolution layer width D_A with different ultrasonic durations were calculated according to the equation shown below.

$$D_A = [(D_1 - d_1) + (D_2 - d_2) + \ldots\ldots + (D_N - d_N)] / N \quad (1)$$

where D_A is the dissolution layer, D is the width of the liquid region, d is the distance between the base materials, and N is the number of measurements ($N > 8$).

When ultrasonic duration was 2 s, most of the oxide films were still continuously distributed along with the interface and almost the interlayer was still solid. Because the continuous oxide films blocked the element diffusion and the generation of low-temperature Zn-Al eutectics. The distance d between the two-side interfaces was shorter than the thickness of the original Zn foil. Because the Zn interlayer softened at the welding temperature, and the distance between the base materials was significantly reduced under constant pressure and ultrasonic extrusion. The width of the dissolution layer $D_{A\text{-}2s}$ is 0 μm, which meant no diffusion layer occurred. With applying ultrasonic vibration for 5 s, the interfacial oxide film was partially broken. The aluminum in the base MMCs migrated into the intermediate layer via micro-channels generated by the partial fracture of the oxide film. The width of the dissolution layer $D_{A\text{-}5s}$ increased to 40 μm. The microstructure of the bonding zone was consisted of gray dendritic α-Al, white globular β-Zn, and Zn-Al eutectic. This kind of Zn-Al alloy microstructure meant the pure zinc interlayer was transited to low-temperature Zn-Al eutectic and took further element-diffusion within only 5 s. With increasing ultrasonic duration to 20 s, the original oxide film on the surface of the composites had been completely removed. The materials near the interface and interlayer zone were fully liquefied and mutually dissolved. The width of the dissolution layer $D_{A\text{-}20s}$ increased to 90 μm. Some mini-size SiC particles near the interface began to move towards the bonding zone, while the middle-size and large-size SiC particles did not move significantly. With prolonging ultrasonic vibration time to 40 s, the dissolution and diffusion of elements went further, and the dissolution area increased significantly. The width of the dissolution layer $D_{A\text{-}40s}$ reached 105 μm. The fine elliptic α-Al distributed evenly in the bonding zone. A large number of mini-size SiC particles entered the bonding zone and dispersed evenly. Meanwhile, the middle-size SiC particles near the interface moved in the bonding zone due to the melting of the surrounding substrate. Figure 6 shows the D_A values with different ultrasonic duration. The slope of the curve was first increased and then decreased with the prolonging ultrasonic vibration. That indicated the effect of ultrasound on promoting elements dissolution was more significant when the ultrasonic duration was 5 ~ 20 s.

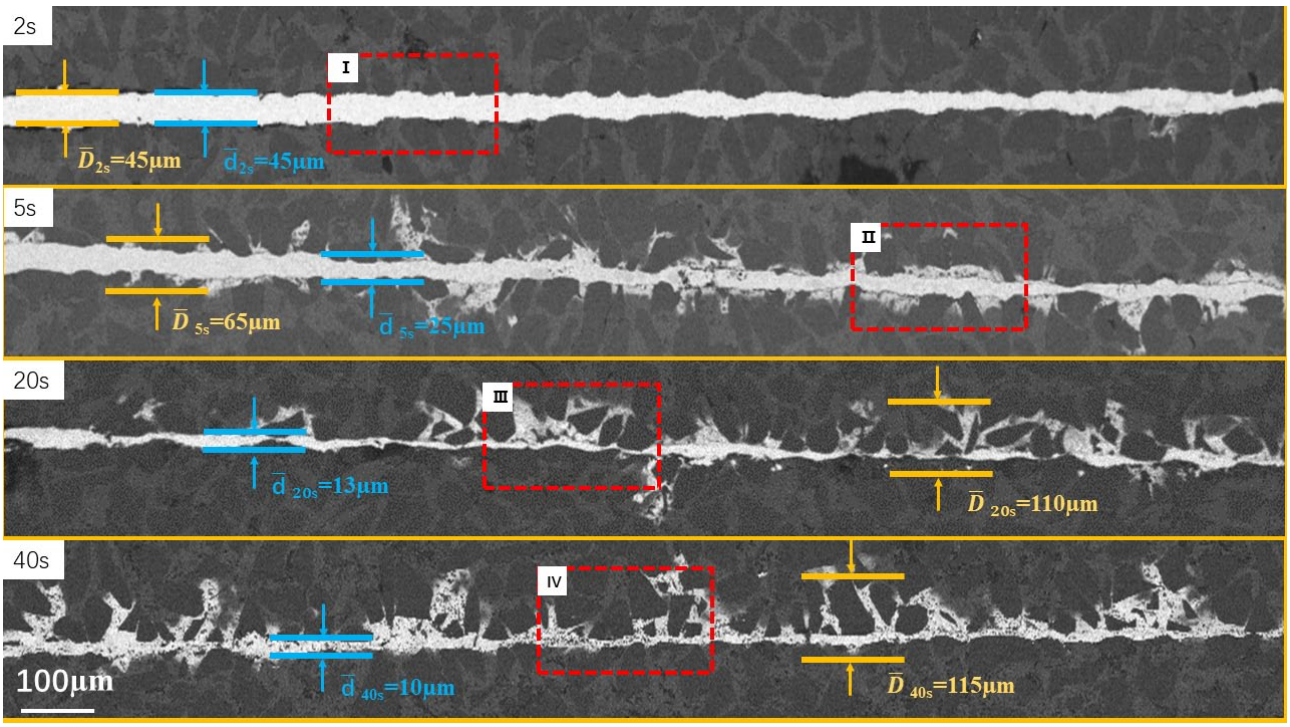

Fig. 4. The interface macroscopic morphology of SiCp/Al MMCs joint under different ultrasonic application time

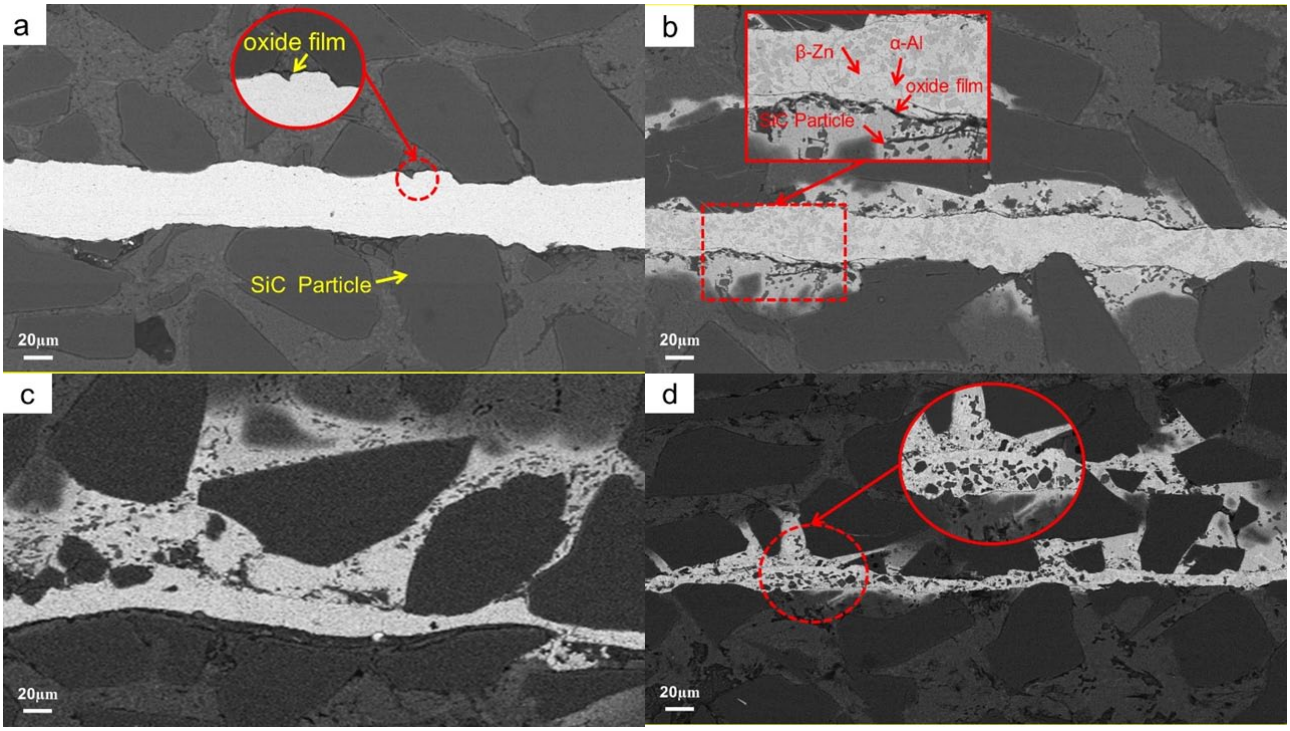

Fig. 5. Microstructure of the bonding seam with the different ultrasonic vibration time (a) With ultrasonic vibration time of 2 s (I zone in Fig. 4), (b) With ultrasonic vibration time of 5 s (II zone in Fig. 4), (c) With ultrasonic vibration time of 20 s (III zone in Fig. 4), (d) With ultrasonic vibration time of 40 s (IV zone in Fig. 4)

The average shear strength of the joints with different ultrasonic duration is shown in Fig. 7. When ultrasonic vibration time was 2 s, the joint separated during the wire cutting process. A small part of the solder was attached to the substrate surface after the separation, which meant that the substrates were locally bonded but the bonding area was too small due to the short ultrasonic action time. With the increased of ultrasonic vibration time, the shear strength of the joints increased. When prolonging ultrasonic vibration time to 40 s, the average shear strength reached 56.34 MPa. The similar effect rules of ultrasonic

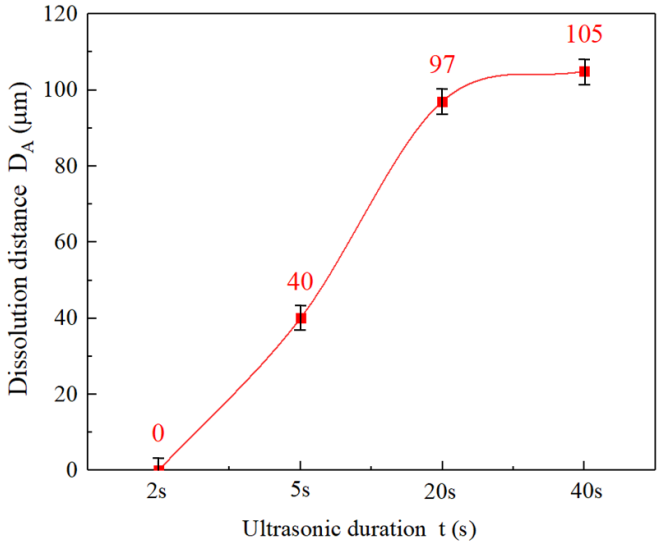

Fig. 6. The average width of the dissolution layer under different ultrasonic application time

duration were obtained in the Al-50 Si alloys bonded by U-TLP [26,35]. With the increased of ultrasonic vibration time, the shear strength of the joints also increased.

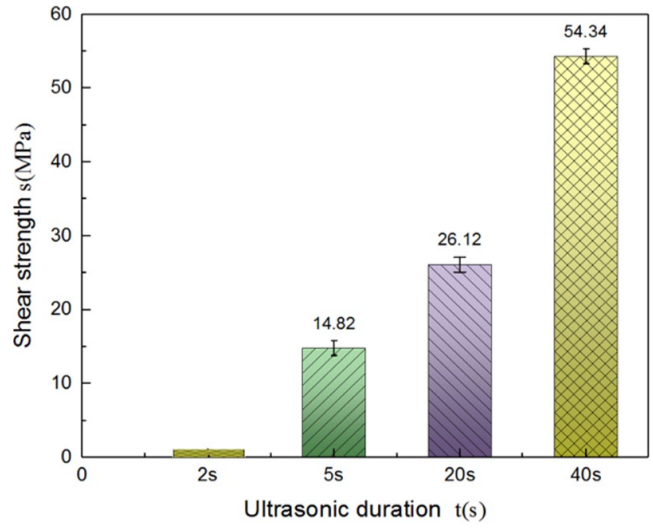

Fig. 7. Shear strengths of bonding with different ultrasonic duration

Fig. 8 shows the fracture morphologies of the joints under different ultrasonic duration, and TABLE 1 shows the contents of different elements of different points in Fig. 8. The joint with 2 s ultrasonic vibration was torn along the interface between the substrate and the intermediate layer. Partial interlayer metal attached to the substrate surface. Typical Zn-Al eutectic pattern and bare SiC particles were observed in the attached area, shown as Fig. 8a, which indicated that local diffusion occurred at that time but the effective bonding was not realized due to the short ultrasonic duration. In Fig. 8b, there were two kinds of phases and three kinds of particles on the fracture surface of the joint applying 40 s ultrasonic vibration, i.e. α-Al and Zn-Al eutectic phase, min-size, big-size, and middle-size SiC particles. Thereto, min-size particles were wrapped in the α-Al and Zn-Al eutectic phase and scattered in the bonding zone (Particles I). The big-size particles moved towards the bonding area but did not pass through the bonding zone (Particles III). Middle-size particles separated from the base metal and moved into the bonding zone (Particles II). That indicated some middle-size particles entered the bonding zone, consistent with the microstructure in Fig. 5.

TABLE 1

EDX component analysis of points in Fig. 8 (wt %)

Point	The contents of different elements				
	Al	Zn	Si	C	Others
A	4.25±0.23	72.12±3.43	15.38±0.36	7.78±0.88	0.47
B	1.47±0.17	1.72±0.11	66.18±1.76	22.43±1.19	8.80
C	23.43±1.12	45.44±1.73	14.33±0.33	9.34±0.92	7.46
D	2.76±0.19	3.35±0.21	65.26±1.56	22.98±1.18	5.65
E	1.15±0.11	0.76±0.14	72.54±1.81	23.74±1.20	1.81
F	2.01±0.13	4.75±0.23	71.13±1.77	15.12±1.35	7.99
G	4.50±0.21	67.47±3.12	16.90±0.43	5.53±0.46	5.60

4. Discussion

To investigate the role of ultrasound in the transient liquefaction stage, according to the process and characters of the transient liquefaction stage of U-TLP, we discussed the effects of ultrasound deeply from three issues i.e. the effects on oxide

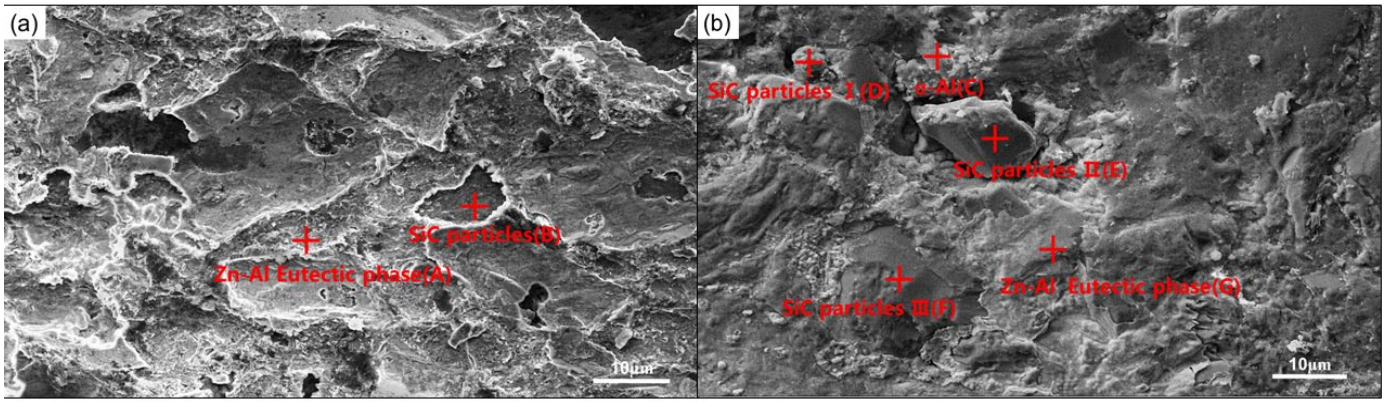

Fig. 8. The fracture surface microstructure morphology of bonding with different ultrasonic vibration time of (a) 20 s, (b) 40 s

films, interface microstructure evolution, and the migration and distribution of SiC particles. Based on the effects of ultrasound which were covered here, the physical model of the ultrasonic action process in the transient liquefaction stage was formulated.

4.1. Effects of ultrasonic vibration on the oxide film

Oxide film removal was one of the key points in the research of aluminum matrix composite bonding in air. The significant effects of ultrasound on removing oxide film in ultrasound-assisted brazing have been evaluated in details [20]. In the brazing process, the oxide film breaking mechanism was the ultrasonic cavitation effect generated in the liquid filler metal. The removal process of oxide film was to melt the filler metal first. After forward, the ultrasonic cavitation bubbles generated and destroyed the oxide film. The requirement of cavitation construction was the existence of liquid. In the U-TLP process, However, oxide film removed was the requirement before the low-temperature eutectic generation. At the beginning of ultrasound application (within 2 s), most of oxide films were still continuously distributed on the interface. Partial oxide film cracked because of the high-frequency longitudinal vibration and transverse friction which were induced by ultrasound [26]. Only rare low-melting Zn-Al eutectic generated due to the limited cracks and diffusion time. This period could be named as mechanical break period of oxide removal. As prolonging the ultrasonic time, more liquid eutectics formed due to more cracks of oxide films and more sufficient diffusion between Zn and Al atoms. As the formation of enough liquid eutectic, the ultrasonic cavitation effect began playing the main role of breaking and removing the left oxide films. This period was the basically same as oxide films breaking in ultrasonic-assisted brazing. It could be named as cavitation induced removal period of oxide films, which could accomplish within 20 s. We tried to bond the SiCp/Al MMCs at 390°C with heat preservation time 120 s in the prior work, however, without ultrasonic vibration the oxide films were not destroyed apparently, and elements did not diffuse under heating (390°C) and pressing (1.5 MPa) in the air environment [33].

Noteworthily, a particular phenomenon was found in this study. After the complete removal of original oxide films, a kind of new root-whisker-like oxide formed near the bonding interface and SiC particles (as shown in Fig. 9). Based on the component identification, this kind of rootlike oxide was composed of zinc, aluminum, silicon, carbon, and oxygen, as shown in TABLE 2. The component of this new oxide was significantly different from the original oxide films Al_2O_3. Besides, this rootlike oxide still existed when prolonging ultrasonic duration. While, the new oxide became thinner and smaller as shown in Fig. 9b. According to the condition of the chemical reaction and the atomic percentage in TABLE 1, we inferred the new oxide was a kind of C-ZnO compound in which contained few Al_2O_3. The source of these elements was the key to explain why this new compound is formed. Zinc was easy to obtain from the Zn interlayer. Carbon comes from the graphite added in the high-temperature sintering experiment during the preparation of the matrix [33]. Oxygen may mainly come from the air in the process of experiment. In the early stage of transient liquefaction, when the interlayer metal was changing from solid to liquid, and the oxygen located near the interface could permeate into the bonding zone and reacted with Zn and C undergoing the effect of pressure and heat. Finally, C-ZnO formed as a brittle rhizome carbon oxide. Besides, this rootlike C-ZnO still existed when prolonging ultrasonic duration. While the new oxide became thinner and smaller as shown in Fig. 8b. The revolution of C-ZnO was induced by ultrasonic effect. Firstly, the C-ZnO compounds were shattered by ultrasonic cavitation and were evenly stirred in the joint area due to the mixture effect of ultrasonic streaming. Then, the carbon oxide

TABLE 2

Composition of the new component in different points (wt %)

Element	Point 1	Point 2	Point 3
C	57.73±3.45	53.31±2.78	56.98±3.11
O	19.91±1.34	20.88±1.39	19.70±1.28
Al	3.38±0.21	4.01±0.23	3.54±0.18
Si	2.31±0.18	2.55±0.17	3.01±0.21
Zn	15.13±0.81	17.33±0.77	15.55±0.75
Others	1.54	1.92	1.22

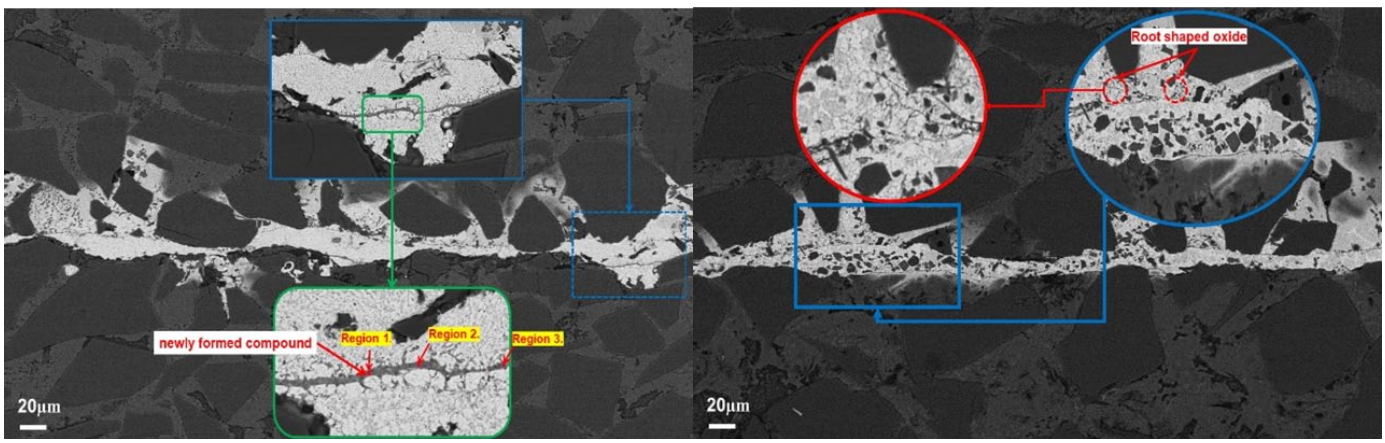

(a) (b)

Fig. 9. Microstructure of the bonding seam with the ultrasonic vibration time of (a) 20 s, (b) 40 s

reacted with carbon, oxygen, and zinc in the bonding zone continually and grew as the new C-ZnO components.

4.2. Effects of ultrasonic vibration on microstructure evolution

The evolution of the microstructure of the bonding area directly influenced the bonding quality. The microstructure evolution of SiCp/Al MMCs joint undergoing U-TLP can be described as follows. Firstly, before triggering ultrasonic vibration, the base MMCs and the zinc foil formed a tight sandwich structure. With the application of ultrasonic vibration, part of the oxide films broke i.e. the mechanical breaking period (mentioned in section 4.1). At that moment, ultrasonic provided activation energy for metal atoms and accelerated the dissolution and diffusion [26]. The aluminum in the MMCs and the zinc in the intermediate layer diffused rapidly through the micro-channel generated by the partial breakdown of the oxide film. As the ultrasonic duration increased, the Zn-Al eutectic with a low melting point filled up the bonding zone and melted at the welding temperature. Finally, under the effect of ultrasonic vibration, more aluminum dissolved into bonding, the dendritic α-Al broke into more refined grains under the influence of ultrasound, and the local formation of the solid phased structure of α-Al at the bonding temperature. And the dissolution layer between Zn interlayer and base material gradually widened. During the cooling period, a part of β-Zn precipitated from α-Al. In summary, the microstructure of the bonding zone after the transient liquefaction stage was a typical Zn-Al alloy microstructure, which consisted of α-Al, white β-Zn, and some Zn-Al eutectic phases. Besides, the width of the intermediate layer decreased gradually with the increase of ultrasonic duration, because static pressure and high-frequency ultrasonic vibration extruded out some of the liquid phases.

4.3. Effects of ultrasonic vibration on migration and distribution of SiC particles

The distribution of SiC particles, including three size particles in this study, is another critical factor affecting the bonding quality of high-volume fraction particle reinforced aluminum matrix composites. At the early stage of the bonding process in this paper, because of the short ultrasonic vibration time, Al alloy matrix around SiC particles did not melt, the SiC particles couldn't move. As the ultrasonic duration increased, the base metal near interface melted and the mini-size SiC particles in the liquid area trended to move driven by acoustic streaming [32]. Due to the barrier effect of the oxide film, the particles could not move into the intermediate zone. They just concentrated in the vicinity of the oxide film. We named this period "*the limited active stage*". With the ultrasonic vibration prolonging, local oxide film removed. The mini-size SiC particles were surrounded by the liquid phase and entered the intermediate zone driven by acoustic flow. We call it "*locally moving stage*". When the oxide film was completely broken, a large number of mini-size SiC particles entered the whole bonding zone and distributed evenly with the action of acoustic streaming. As the intermediate layer melting, the dissolution rate increased rapidly and the liquid area extended toward base metal under the effect of ultrasound. At that moment, the middle-size SiC particles closed to the weld zone began to move to the center of the bonding zone. Although some large-size particles have moved, they have not moved into the joint area. This stage was called "*The even distribution stage*". As a large number of particles entered the whole bonding zone and distributed evenly, SiC particles played a certain role in pinning effect and promoting nucleation. These effects can improve the segregation of particles. The middle-size SiC particles could effectively bear the load of the bonding zone and prevent crack extension in the shear test, thereby increasing joint strength in disguised form. This period was similar to ultrasonic-assisted brazing of particle reinforced aluminium alloy [26,32,35]. For the conventional TLP without ultrasonic vibration, a small number of particles near the interface enter the bonding zone slowly in the transient liquefaction stage (TLS). And without the acoustic streaming of ultrasonic, SiC particles could not be distributed evenly in the bonding. As the solidification process goes on, particle segregation occurred in the bonding zone [36].

4.4. Physical model of ultrasonic action process

Based on the detailed discussion of the effects of ultrasound on the fracture of the oxide film, the evolution of microstructure, and the homogenization of SiC particles, the physical process of ultrasonic action in the transient liquefaction stage were summarized. The process mainly included six stages, as shown in Fig. 10.

Stage 1: Before ultrasonic vibration was applied, the SiCp/Al MMCs and the Zinc foil were formed as a compact sandwich structure. Due to the obstruction of the oxide film, there was no element diffusion between the base material and the intermediate layer.

Stage 2: During the initial short time of ultrasonic applying, under preset static pressure and ultrasonic vibration, the local oxide films cracked by transverse friction and longitudinal high-frequency ultrasonic vibration [26]. Meanwhile, the rapid diffusion between zinc and aluminum began via the microchannel under ultrasound promotion [33].

Stage 3: When the composition near the interface reached the eutectic component point, the eutectic reaction occurred. The formed Zn-Al low-temperature eutectic melted at the bonding temperature (390°C) [34].

Stage 4: With the continuous ultrasonic vibration, the cavitation effect was formed in the local eutectic liquid at this time. The cavitation bubbles produced high-temperature and high-pressure micro-jet which can rapidly break the surrounding oxidation film. The more the oxide films was destroyed, the faster elements dissolution happened, and

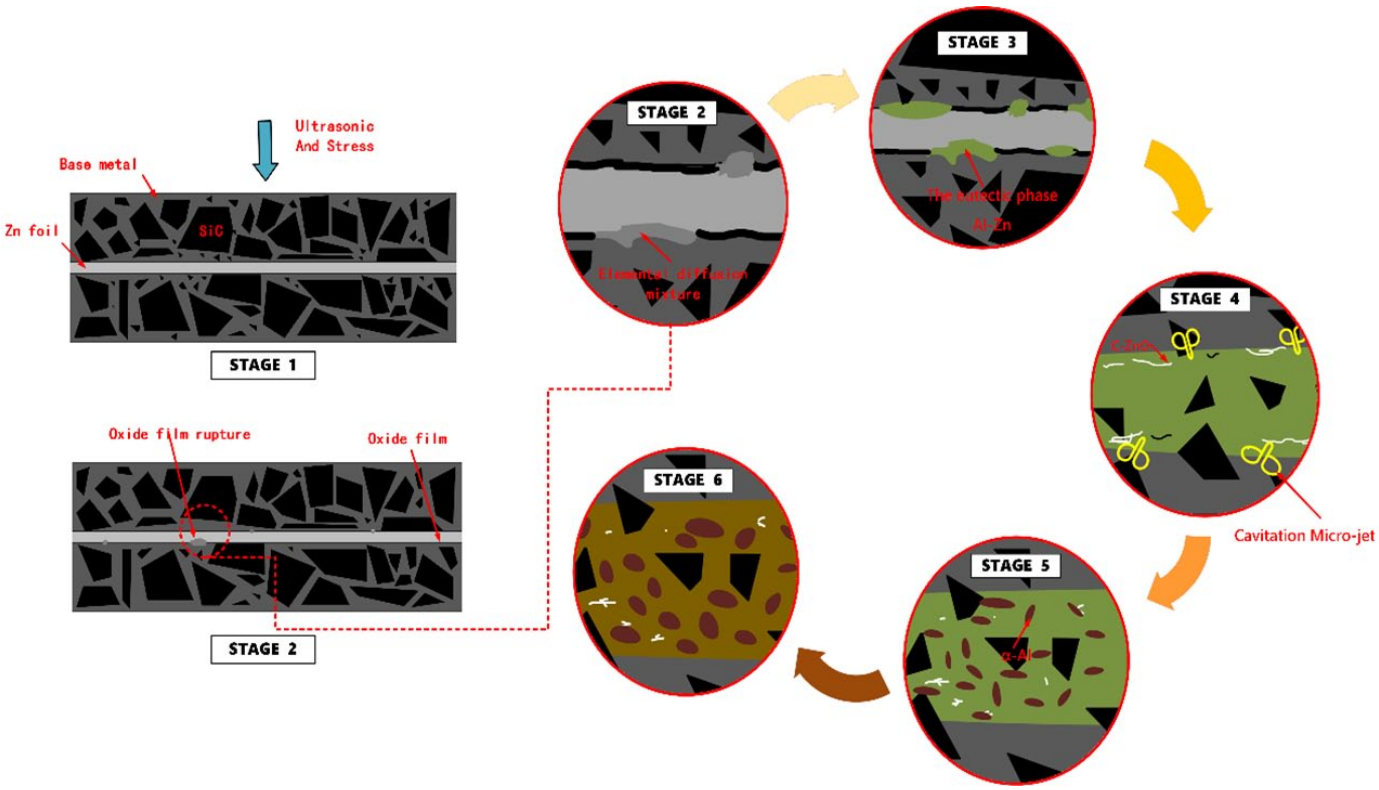

Fig. 10. Joint formation mechanism between SiCp/Al MMCs U-TLP and zinc layer

the more liquid phase was formed. During this process, the weld metal was gradually melted to complete liquid. Besides, in the region where the oxide film disappeared, a new rootlike C-ZnO compound was formed.

Stage 5: As ultrasonic duration increased, rapid dissolution and diffusion continued between the residual liquid phase and the base metal. Aluminum increased in the bonding area and the dendritic α-Al solid-phase began to precipitate. The precipitated α-Al-phases were refined to a certain extent due to the effect of ultrasonic cavitation on promoting nucleation and breaking dendrite. Meanwhile, the newly formed C-ZnO compound became the thinner rootlike shape.

Stage 6: After stopping ultrasonic vibration and heating, direct water quenching kept the microstructure of the transient liquefaction stage. When the U-TLP process was completed, the bonding zone mainly consisted of a relatively uniform distribution of α-Al phases, the β-Zn precipitated phases, the eutectic phase Al-Zn and evenly distributed SiC particles.

5. Conclusions

The welding of high-volume SiC particle reinforced aluminum matrix composites was realized by applying U-TLP bonding technology and intermediate zinc layer in the atmospheric environment. The main conclusions are as follows:

(1) U-TLP can realize the good combination of high volume SiCp/Al MMCs in the atmospheric environment and low temperature (390°C). A complete joint was formed at 40 seconds of ultrasonic vibration. The shear strength of the joint was 56.34 MPa.

(2) Ultrasonic vibration can break and remove the oxide film, the oxide film was cleared entirely at 20 s of ultrasonic vibration. Ultrasonic vibration can also break the newly generated rhizome C-ZnO compounds and make the rhizome C-ZnO compounds uniformly distributed in the joining area.

(3) Ultrasonic vibration can promote the diffusion of elements, and the instantaneous liquefaction of the weld zone can be realized under the action of ultrasonic in a short time (5 s). The microstructure of the weld zone is mainly composed of α-Al, β-Zn, and Zn-Al eutectic structure. With the increase of ultrasonic time, the proportion of spherical Al increases, and the microstructure is finer and more uniform.

(4) With the increase of ultrasonic time, mini-size SiC particles under the action of ultrasonic acoustic flow entered the weld zone and were evenly distributed, and no bias phenomenon occurred. As the nearby liquid phase gradually increasing, middle-size SiC particles also begin to move towards the weld zone to a certain degree, strengthening the joint. The joint break along the base material area near the welding line, which greatly improve the bonding efficiency of SiCp/Al MMCs.

(5) In conclusion, ultrasonic broke down and removed the oxide film through physical vibration, friction and cavitation in the instantaneous liquefaction process, and ultrasonic acoustic flow agitation can promote the uniform distribution of tissues, strengthen the joint, and establish the physical model of U-TLP bonding technology process.

Acknowledgments

Funding: This research was sponsored by the National Natural Science Foundation of China (grant number 51705338), Liaoning Natural Science Foundation (grant number 20180550471), Liaoning Education Department Sci. & Tech. Project(grant number L201731).

REFERENCES

[1] O. Beffort, S. Long, C. Cayron, J. Kuebler, P.A. Buffat, Compos. Sci. Technol. **67**, 737-745 (2007).
[2] D. Lloyd, Int. Mater. Rev. **39**, 1-23 (1994).
[3] M.B.D. Ellis, Int. Mater. Rev. **41**, 41-58 (1996).
[4] D. Storjohann, O.M. Barabash, S.A. David, P.S. Sklad, E.E. Bloom, S.S. Babu, Metall. Mater. Trans A. **36**, 3237-3247 (2005).
[5] Z.Y. Ma, A.H. Feng, B.L. Xiao, J.Z. Fan, L.K. Shi, Mater. Sci. Forum. **539-543**, 3814-3819 (2007).
[6] O.T. Midling, Ø. Grong, Key. Eng. Mat. **104-107**, 355-372 (1995).
[7] T. Yue, J. Xu, H. Man, Appl. Compos. Mater. **4**, 53-64 (1997).
[8] R. Gürler, J. Mater. Sci. Lett. **17**, 1543-1544 (1998).
[9] X.-P. Zhang, L. Ye, Y.-W. Mai, G.-F. Quan, W. Wei, Compos. Part A-Appl. S. **30**, 1415-1421 (1999).
[10] A. Urena, M. Escalera, L. Gil, Compos. Sci. Technol. **60**, 613-622 (2000).
[11] H. Wang, Y. Chen, L. Yu, Mat. Sci. Eng. A-Struct. **293**, 1-6 (2000).
[12] D. Storjohann, O. Barabash, S. David, P. Sklad, E. Bloom, S. Babu, Metall. Mater. Trans. A. **36**, 3237-3247 (2005).
[13] H. Uzun, Mater. Design. **28**, 1440-1446 (2007).
[14] W. Xi-he, N. Ji-tai, G. Shao-kang, W. Le-jun, C. Dong-feng, Mat. Sci. Eng. A-Struct. **499**, 106-110 (2009).
[15] M. Bahrami, K. Dehghani, M.K.B. Givi, Mater. Design. **53**, 217-225 (2014).
[16] T. Prater, Acta. Astronaut. **93**, 366-373 (2014).
[17] V. Patel, S. Bhole, D. Chen, D. Ni, B. Xiao, Z. Ma, Mater. Design. **65**, 489-495 (2015).
[18] Y. Zhai, T.H. North, J. Serrato-Rodrigues, J. Mater. Sci. **32**, 1393-1397 (1997).
[19] J.-h. Huang, Y.-l. Dong, Y. Wan, X.-k. Zhao, H. Zhang, J. Mater. Process. Tech. **190**, 312-316 (2007).
[20] J. Yan, Z. Xu, L. Shi, X. Ma, S. Yang, Mater. Design. **32**, 343-347 (2011).
[21] G. Zhang, Z. Wei, B. Chen, B. Chen, J. Mater. Eng. Perform. **26**, 5921-5937 (2017).
[22] G. Zhang, B. Chen, M. Jin, Mater. Trans. **56**, 212-217 (2015).
[23] Z. Huang, Ultrason. Sonochem. **43**, 101-109 (2018).
[24] X.P. Zhang, G.F. Quan, W. Wei, Compos. Part A-Appl. S. **30**, 823-827 (1999).
[25] J. Niu, X. Luo, H. Tian, J. Brnic, Mater. Sci. Eng. B-Adv. **177**, 1707-1711 (2012).
[26] Q. Wang, X. Chen, L. Zhu, J. Yan, Z. Lai, P. Zhao, J. Bao, G. Lv, C. You, X. Zhou, Ultrason. Sonochem. **34**, 947-952 (2017).
[27] Z.W. Xu, Z.W. Li, L.M. Peng, J.C. Yan, Mater. Design. **161**, 72-79 (2019).
[28] Z.W. Lai, R.S. Xie, C. Pan, X.G. Chen, L. Liu, W.X. Wang, G.S. Zou, Mater. Lett. **166**, 219-222 (2015).
[29] Z.W. Lai, R.S. Xie, C. Pan, X.G. Chen, L. Liu, W.X. Wang, G.S. Zou, J. Mater. Sci. Technol. **33** (6), 567-572(2016).
[30] Z. Lai, X. Chen, C. Pan, R. Xie, L. Liu, G. Zou, Mater. Lett. **166**, 219-222 (2016).
[31] Z.W. Xu, L. Ma, J.C. Yan, S.Q. Yang, S.Y. Du, Compos. Part A-Appl. S. **43** (3), 407-414 (2012).
[32] Z.W. Xu, L. Ma, J.C. Yan, S.Q. Yang, Mater. Chem. Phys. **148** (3), 824-832 (2014).
[33] L. Ma, C.Z. Zhou, Q. Wen, M.S. Li, H. Zhong, S.D. Ji, Ultrasonics. **106**, 106159 (2020).
[34] Z.W. Xu, J.C. Yan, B.Y. Zhang, X.L. Kong, S.Q. Yang, Mat. Sci. Eng. A-Struct. **415** (1-2), 80-86 (2006).
[35] L. Zhu, Q. Wang, L. Shi, X. Zhang, T.H. Yang, J.C. Yan, X.Y. Zhou, S.Y. Chen, Mat. Sci. Eng. A-Struct. **711**, 94-98 (2018).
[36] J. Maity, T.K. Pal, R. Maiti, J. Mater. Sci. **45**, 3575-3587 (2010).